Comparative Performance of TCSC and Wind Energy Integration on Nigerian 48-Bus Grid Using Brown Bear Optimization and Genetic Algorithm

[1]Olusola J. Oyedele, [2]Ganiyu A. Ajenikoko, [2]Isaiah G. Adebayo

[1]Department of Electrical and Electronic Engineering, Bowen University Iwo, Osun State, Nigeria

[2]Department of Electronic and Electrical Engineering, Ladoke Akintola University of Technology, Ogbomoso, Oyo State, Nigeria

Abstract

Introduction: The Nigerian 330 kV transmission system faces persistent operational challenges, including high active power losses, voltage instability, and severe vulnerability to line contingencies, particularly at long, weakly compensated terminal corridors.

Objectives: This study comparatively evaluates series reactive compensation via a Thyristor-Controlled Series Capacitor (TCSC) against localized active/reactive power injection via a Wind Energy Conversion System (WECS) for loss minimization, voltage profile enhancement, and N-1 contingency resilience on the Nigerian 48-bus, 330 kV grid.

Methods: The 48-bus network (1 slack bus, 15 PV buses, 32 PQ buses, 79 lines) was simulated by Newton-Raphson load flow. Brown Bear Optimization (BBO) and a Genetic Algorithm (GA) independently sited and sized each device by minimizing a weighted objective combining normalized real power loss and a Voltage Deviation Index (VDI). All 79 lines were then screened for N-1 contingency severity under the base case and both compensated configurations.

Results: The baseline load flow gave active/reactive losses of 67.702 MW / 2,122.31 MVAr (VDI = 0.02618), with statutory violations at Sakete (0.9255 pu), Kano (0.9471 pu), and Jos (0.9495 pu). Wind integration (100 MW, 100 MVAr) at Sakete reduced active loss by 12.816% and VDI to 0.02170, restoring both Sakete and Jos to compliance. TCSC-BBO, sited on Line 31–33, reduced active loss by 0.396% and restored Sakete's voltage to 0.9576 pu; TCSC-GA, sited on the electrically distant Line 23 (11–13), reduced active loss by a comparable 0.589% but left Sakete's voltage effectively unchanged at 0.9255 pu. GA converged faster than BBO throughout, while both reached similar objective values. Screening identified eight critical N-1 contingencies — including the line carrying the TCSC — that neither compensation strategy resolved.

Conclusions: Localized wind-based active/reactive injection outperforms TCSC series compensation on this network for both loss reduction and voltage recovery, but neither single-device strategy addresses the network's underlying N-1 structural vulnerability, which requires multi-device planning or targeted reinforcement.

Keywords: Nigerian 330 kV grid, Thyristor-Controlled Series Capacitor, Wind Energy Conversion System, Genetic Algorithm, Brown Bear Optimization, N-1 contingency.

1. Introduction

The continuous growth of industrial, commercial, and domestic electricity demand has placed unprecedented stress on transmission networks worldwide. The developing economies feel this most acutely, where structural grid deficiencies, long radial transmission lines, and heavy reliance on centralized generation compound the problem. In Nigeria, generation is concentrated at southern gas-fired stations while major load centres are located far to the north and west, so power must traverse long, weakly meshed lines before reaching demand areas, which leaves the network operating close to its voltage and thermal limits under normal peak conditions [1], [2].

The Nigerian 330 kV network is particularly exposed to this pattern. As power travels these long corridors, inductive line reactance produces significant voltage drop and active power loss [2]. Standard operating criteria require bus voltage magnitude to remain within 0.95 pu ≤ V ≤ 1.05 pu, yet repeated load-flow studies of the network report sub-statutory voltages at terminal buses such as Sakete, Kano and Jos under normal loading [1], [2]. Recent studies confirm this pattern persists on the same network: metaheuristic-tuned UPFC compensation on a comparable Nigerian 330 kV, 56-bus model [24], comparative voltage-stability-limit assessments using multiple prediction optimizers [25], recurring grid-collapse analyses attributing outages to inadequate reactive support [27], and security-optimization studies on this same 48-bus network specifically [28] all report the same terminal-bus vulnerability.

Two broad technical responses exist. The first works within the transmission system itself: FACTS controllers such as the Thyristor-Controlled Series Capacitor (TCSC) alter the effective impedance of a line to regulate power flow and support terminal voltage, and prior work on this same network has shown that TCSC compensation improves local voltage and transient response without requiring new generation construction [3]. SVC-based reactive compensation, tuned via a Genetic Algorithm, has similarly been shown to improve steady-state voltage stability on this same 330 kV network [4], and multi-objective GA-based TCSC siting has more broadly been shown effective for congestion relief and loss reduction beyond the Nigerian context [5]. More recent metaheuristic approaches to TCSC placement, including multi-objective grey wolf optimization [19], hybrid optimisation-logic controllers [21], and hybrid FACTS-allocation methodologies [22], continue to report loss and voltage-profile gains on non-Nigerian test networks, while a direct series-versus-shunt FACTS comparison on this same Nigerian 330 kV system [26] motivates the present TCSC-versus-wind comparison. The second strategy adds generation at the point of need: siting wind or solar capacity at a weak bus supplies active and reactive power locally, which has been shown on the Nigerian grid to relieve line loading and improve voltage stability more directly than series compensation alone, particularly as renewable penetration increases [6]. Independently optimized wind and solar DG placement has achieved similar loss and voltage-stability gains on distribution networks elsewhere [7], and recent reviews and hybrid-metaheuristic case studies continue to confirm that siting choice, not DG capacity alone, drives the benefit [8], [9].

Despite the distinct physical mechanisms of TCSC and wind-based compensation, a direct, like-for-like comparison of the two—sited and sized independently under a shared objective function and stress-tested against the same contingency set remains uncommon on an updated model of the Nigerian grid. Because optimal device placement is a non-linear, non-convex combinatorial problem, metaheuristic search is required to avoid local-optima traps. This study uses both a Genetic Algorithm and the more recently proposed Brown Bear Optimization algorithm, which models the pedal scent-marking and territorial behaviour of brown bears to balance exploration and exploitation and has performed competitively against established methods on economic-dispatch and structural-optimization benchmarks [10], [11], and has more recently been applied to load-frequency control of renewable-integrated power systems [20]. Comparable metaheuristic approaches, including whale-optimization-based joint siting of multiple FACTS device types, report similar gains when the search is left free to find its own trade-off between loss and voltage objectives [12]. Using both algorithms independently on the same problem also guards against either search reporting a false optimum caused by premature convergence.

Voltage stability on this network has been well documented: Okakwu et al. [2] found that terminal buses without adequate reactive support consistently fall below the statutory threshold under normal peak loading, and related contingency and transfer-capability studies have shown that single-line outages on electric lines can push the system into a non-convergent or infeasible operating state, indicating voltage collapse, rather than a merely severe but recoverable experience [13]. On the compensation side, Okakwu et al. [3] found that TCSC placement measurably improves the terminal voltage and transient response near the compensated line, while Adetokun et al. [6] found that renewable injection directly at load-proximate buses improves voltage stability indices more effectively than transmission-level compensation alone as penetration increases. This is consistent with wind-resource assessments showing that Nigeria's northern network, where Kano sits, holds genuinely strong wind potential that has gone largely untapped for grid support [14]. Evaluating network resilience separately requires contingency analysis: standard practice re-solves the AC load flow with each line removed in turn and flags non-convergence as an indicator of voltage collapse, since an AC solution captures voltage impacts that a DC or linearized screening cannot [13], a principle reflected in recent modern stability-assessment indices developed specifically for contingency ranking [23], and studies of this kind on the Nigerian grid have repeatedly found that a small number of radial, single-point-of-failure account for most severe contingencies on a large network.

2. Objectives

This paper's specific objectives are to: (i) establish a baseline Newton-Raphson load flow of the 48-bus, 79-branch Nigerian grid and identify its weak buses; (ii) formulate and minimize a multi-objective function combining real power loss and the Voltage Deviation Index; (iii) compare the placement and sizing of TCSC and wind resources found independently by Brown Bear Optimization and a Genetic Algorithm; and (iv) screen all 79 lines for N-1 contingency severity and assess whether either single-device compensation strategy changes the network's exposure to critical outages.

3. Methods

System Description and Baseline Load Flow

The network comprises 1 slack bus (Shiroro GS), 15 PV buses, 32 PQ buses, and 79 transmission lines, with bus and branch data following the Nigerian 330 kV, 48-bus system reported by Nkan et al. [1]. The active and reactive power injections at bus i are

$$P_i = V_i \sum_{j=1}^{N_b} V_j \left(G_{ij} \cos\theta_{ij} + B_{ij} \sin\theta_{ij}\right) \qquad (1)$$

$$Q_i = V_i \sum_{j=1}^{N_b} V_j \left(G_{ij} \sin\theta_{ij} - B_{ij} \cos\theta_{ij}\right) \qquad (2)$$

where V_i and V_j denote bus voltage magnitudes, $\theta_{ij} = \delta_i - \delta_j$ represents the phase angle difference, $N_b = 48$ is the total bus count, and $G_{ij} + jB_{ij}$ represents the (i, j)-th element of the bus admittance matrix (Y_{bus}).

Load flow solutions are obtained using the Newton-Raphson iterative scheme initialized from a flat start ($V = 1.0$ pu, $\delta = 0°$). System convergence is governed by power mismatch vectors solving the linearized matrix equation:

Convergence is achieved when the maximum absolute power mismatch falls below a strict tolerance threshold of 10^{-6} pu, following the standard formulation [15].

TCSC Modeling

The TCSC is represented as a controllable series reactance on a candidate line. For a device on line k connecting bus i and bus j, the adjusted branch reactance, following the reactance-injection model of [29], is

$$X_{ij}, new = X_{ij} + X_{TCSC} = (1 + r) \cdot X_{ij} \qquad (3)$$

where r = X_{TCSC} / X_{ij} is the degree of series compensation, bounded within −0.70 ≤ r ≤ 0.15 to avoid the resonance-prone region near full reactance cancellation. The location and compensation ratio were searched jointly, in a single stage. The TCSC control based on the firing angle is inherently included in the model through its variation within the specified range. For every iteration of the optimization process, the relevant entries of the matrix are adjusted accordingly, and a modified Newton-Raphson load flow is resolved to obtain the new steady-state solution for that candidate.

Wind Energy Conversion System Modeling

The wind unit is modeled as a fixed-capacity active/reactive injection at a candidate bus m,

$$P_{m,\text{net}} = P_{m,\text{load}} - P_{\text{Wind}} \qquad (4)$$

$$Q_{m,\text{net}} = Q_{m,\text{load}} - Q_{\text{Wind}} \qquad (5)$$

with $P_{\text{Wind}} = 100$ MW and $Q_{\text{Wind}} = 100$ MVAr. Allowing reactive supply independent of active supply lets the unit act as a local voltage-support device as well as an energy source, which is a distinction; as Section 4 shows, it is the reactive rather than the active injection that ultimately restores the weakest bus to its statutory band.

Objective Function

Both device types were sited and sized by minimizing a weighted composite objective:

$$J = w_1 \left(\frac{P_{\text{loss}}}{P_{\text{loss, base}}}\right) + w_2 \left(\frac{\text{VDI}}{\text{VDI}_{\text{base}}}\right) \qquad (6)$$

with equal weights $w_1 = w_2 = 0.5$. Total active power loss across all L = 79 branches and system-wide VDI are

$$P_{\text{loss}} = \sum_{k=1}^{L} g_k \left[V_i^2 + V_j^2 - 2V_iV_j \cos(\delta_i - \delta_j)\right] \qquad (7)$$

$$\text{VDI} = \sum_{i=1}^{N_b} \left(\frac{V_i - V_{\text{ref}}}{V_{\text{ref}}}\right)^2 \qquad (8)$$

where g_k is the conductance of line k and V_{ref} = 1.0 pu, in the form of classical voltage-stability indicators that quantify proximity to collapse directly from normal load-flow output [16]. A penalty term was added to J whenever any bus voltage fell outside 0.90–1.10 pu in a candidate solution.

Optimization Algorithms and Contingency Screening

Two metaheuristics identified device location and size independently under the same objective function.

The Genetic Algorithm (GA) implementation used MATLAB's Global Optimization Toolbox ga() function, configured with a population size of 30 and a maximum of 100 generations, matching the settings used for BBO to keep the comparison fair. Each candidate solution — a line index and compensation ratio for TCSC, or a bus index with active/reactive injection size for wind — was encoded as a real-valued vector with the location variable constrained to integer values via the toolbox's mixed-integer handling. Selection used the toolbox's default tournament selection, and new generations were formed through crossover and mutation operators applied to the selected parents, following the canonical GA formulation [17]. At each generation, every candidate solution was evaluated by re-solving the full AC Newton-Raphson load flow and computing the composite objective in Eq. (6); the best objective value found up to that generation was logged to produce the convergence curves in Figs. 1 and 2. The algorithm terminated at the fixed generation limit rather than an early-stopping criterion, so that BBO and GA were compared under an identical computational budget.

Brown Bear Optimization (BBO) [10] updates candidate solutions through pedal-mark-following, careful-stepping, and territory-defence phases modeled on brown bear foraging behaviour, later extended to a multi-objective form [11].

Algorithm 1: Pseudocode of BBO [10].

Require: N_{iter}, N_{pop}, D and boundaries of variables.

Ensure: Fitness function $f(P)$ is defined.

Initialize random group of bears

Form population P of group of bears

Initialize best fitness $f^{best} = \inf$ and $k = 1$.

while ($k \leq N_{iter}$) do

for ($i = 1$:size$(P, 1)$) do

Check limit constraints of pedal marks.

Evaluate fitness function $f(P_i)$.

if ($f^{best} > f(P_i)$) then

$f^{best} = f(P_i)$;

$P_k^{best} = P(i, :)$;

end if

end for

\ *Pedal scent marking behavior starts...* \

Select best and worst group of bears.

$\theta_k = \frac{k}{N_{iter}}$;

for ($i = 1$:size$(P, 1)$) do

% *Characteristic gait while walking*

if ($\theta_k > 0$ && $\theta_k \leq \frac{1}{3}$) then

Update $P_{i,k}$

% *Careful stepping characteristics*

4. Results

else if ($\theta_k > \frac{1}{3}$ && $\theta_k \leq \frac{2}{3}$) then

Update $P_{i,k}$ using (6.5).

% *Twisting feet characteristic*

else if ($\theta_k > \frac{2}{3}$ && $\theta_k \leq 1$) then

Update $P_{i,k}$

end if

end for

Select better group of bears.

\ *Pedal scent marking behavior ends...* \

\ *Sniffing behavior starts...* \

for ($m = 1$:size$(P, 1)$) do

Select one random group of bears $P_{n,k}$ where $m \neq n$.

Update $P_{m,k}$ using (6.10).

end for

Select better group of bears.

\ *Sniffing behavior ends...* \

$k = k + 1$;

end while

print f^{best} and P^{best}

Both used a population size of 30 and a maximum of 100 iterations/generations, with the load flow re-solved at every candidate evaluation. Each of the network's 79 lines was then tripped in turn and the network re-solved with the full AC Newton-Raphson iterative load flow; a contingency was applied to determine severe line when the post-outage load flow failed to converge, the standard indicator of voltage collapse following the classical automatic-contingency-selection approach [18] and its application to Nigerian grid [13], and this screening was repeated for the base case and both compensated networks.

Base-Case Load Flow

The baseline Newton-Raphson solution converged with a tolerance of 10^{-6} pu. Active and reactive power losses reached 67.702 MW and 2,122.31 MVAr, respectively, giving a system VDI of 0.02618. Three buses violated the statutory 0.95–1.05 pu band (Table 1): Bus 31 (Sakete, 0.9255 pu), Bus 4 (Kano, 0.9471 pu), and Bus 9 (Jos, 0.9495 pu). Sakete was the most severe violation, consistent with its heavy terminal loading and electrical distance from the nearest generation [1], [2]. The Appendix provides the complete 48-bus voltage solution (Table A1).

Table 1. Buses Violating the ±5% Statutory Voltage Band — Base Case

Bus No.	Bus Name	V (pu)	Angle (deg)	V (kV)
4	Kano	0.9471	-4.6719	312.55
9	Jos	0.9495	-5.3841	313.35
31	Sakete	0.9255	-14.666	305.41

Optimization Performance and Device Allocation

For TCSC allocation, GA converged in 5.48 s against 10.28 s for BBO; for wind allocation, GA converged in 6.14 s against 8.62 s for BBO. Both converged to matching or near-matching objective values, and for wind allocation, both reached the identical global optimum — Bus 31 (Sakete), 100 MW and 100 MVAr, J = 0.44677.

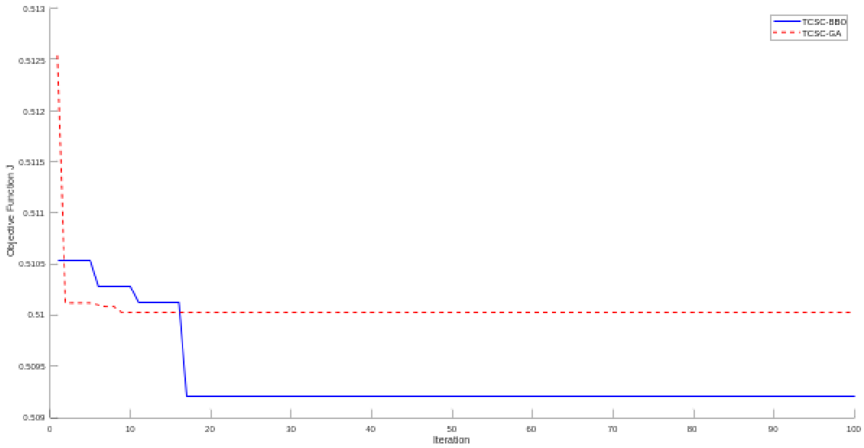

Fig. 1. Convergence characteristics of BBO and GA for optimal TCSC allocation.

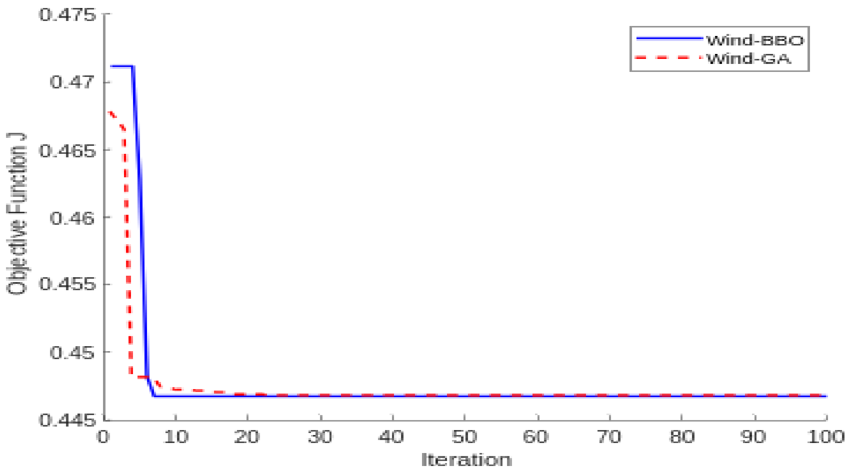

Fig. 2. Convergence characteristics of BBO and GA for optimal wind allocation.

Table 2. Comparative Optimization Results for TCSC and Wind Integration

Method	Location	Size	P_loss (MW)	Loss Red. (%)	Q_loss (MVAr)	VDI	J	Runtime (s)
Base Case	—	—	67.702	—	2,122.30	0.02618	—	—
TCSC-BBO	Line 57 (31–33)	r = −0.700	67.434	0.396	2,105.80	0.02238	0.50921	10.28

Method	Location	Size	P_loss (MW)	Loss Red. (%)	Q_loss (MVAr)	VDI	J	Runtime (s)
TCSC-GA	Line 23 (11–13)	r = −0.433	67.303	0.589	2,115.20	0.02593	0.51002	5.48
Wind-BBO	Bus 31 (Sakete)	P=100,Q=100	59.025	12.816	2,057.90	0.02170	0.44677	8.62
Wind-GA	Bus 31 (Sakete)	P=100,Q=100	59.025	12.816	2,057.90	0.02170	0.44677	6.14

System Loss, VDI, and Voltage Profile

Wind injection at Bus 31 reduced active power loss by 12.816% and reactive power loss by 3.034%, against 0.396–0.589% and 0.335–0.777% for the two TCSC solutions, respectively. TCSC compensation on Line 31–33 restored Sakete from 0.9255 pu to 0.9576 pu, leaving Kano and Jos effectively unchanged. Wind injection restored Sakete to 0.9559 pu and, through broader reactive support, also lifted Jos into compliance at 0.9503 pu; Kano remained marginally below the statutory limit under both options (0.9471–0.9478 pu), pointing to a genuine northern reactive-support gap that neither device — sited to resolve the more severe Sakete violation — was positioned to reach.

Table 3. Weak Bus Voltage Profile Before and After Optimization (pu)

Bus No.	Bus Name	Base Case	Post-TCSC-BBO	Post-Wind	Status
4	Kano	0.9471	0.9471	0.9478	Sub-statutory, both
9	Jos	0.9495	0.9495	0.9503	Resolved via Wind
31	Sakete	0.9255	0.9576	0.9559	Resolved via both

Note: "Post-TCSC-BBO" reflects the TCSC-BBO solution (Line 31–33), which restores Sakete's voltage; TCSC-GA (Line 23, 11–13) is electrically remote from all three weak buses and leaves each essentially at its base-case value (see Section 4, "Optimization Performance and Device Allocation").

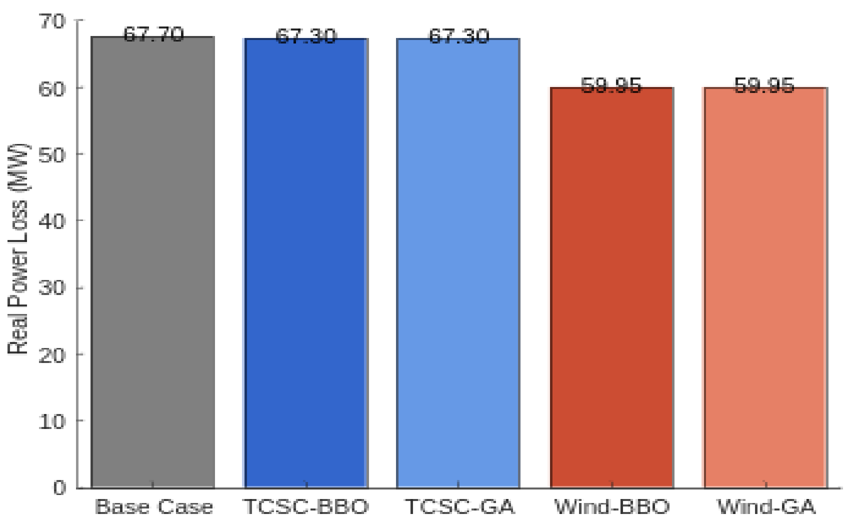

Fig. 3. Real power loss comparison across optimization scenarios.

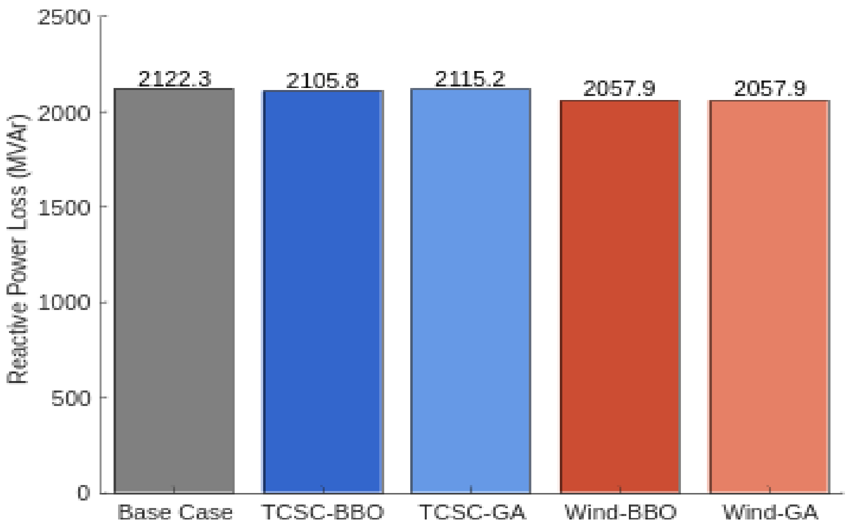

Fig. 4. Reactive power loss comparison and loss reduction (%).

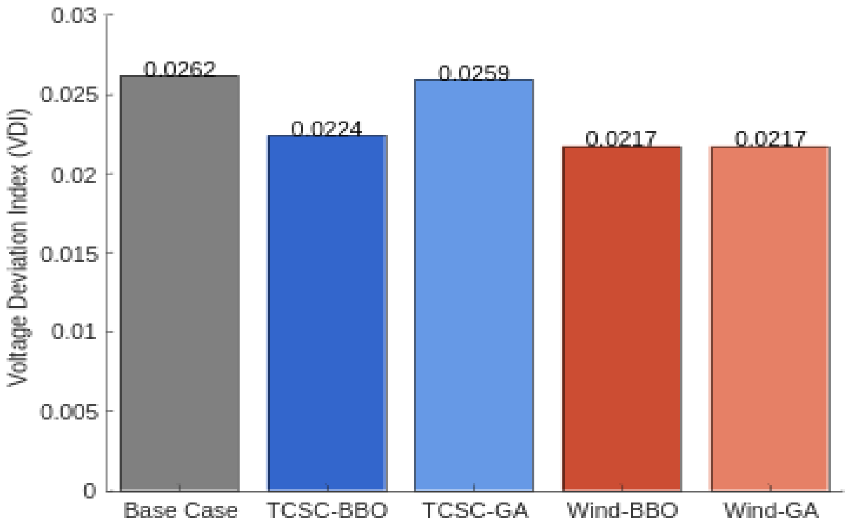

Fig. 5. Voltage deviation index (VDI) comparison.

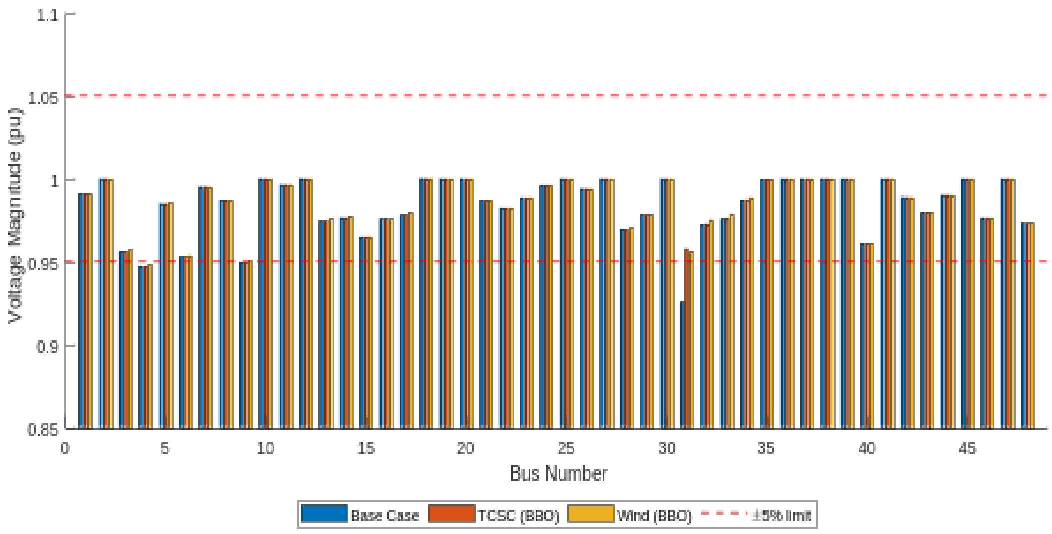

Fig. 6. Voltage profile across all 48 buses: base case vs. TCSC vs. wind.

N-1 Contingency Screening

Contingency screening across all 79 lines identified eight outages that caused power-flow non-convergence under the base case and both compensated configurations (Table 4). A network connectivity check confirmed each is a radial, single-point-of-failure branch that physically isolates part of the network during an outage. Line 57 (31–33) is both one of the eight critical contingencies and the line carrying the TCSC device in the TCSC-BBO solution, so that solution's benefit to Sakete's voltage is contingent on the same line remaining in service.

Table 4. Critical N-1 Contingencies Identified (Base Case, No Device)

Rank	Line	From–To	Corridor	Outcome
1	1	1–2	Birnin Kebbi–Kainji GS	Non-convergent
2	4	3–4	Kaduna–Kano	Non-convergent
3	37	20–26	Odukpani GS–Adiabor	Non-convergent
4	52	26–29	Adiabor–Ikot Ekpene	Non-convergent
5	57	31–33	Sakete–Ikeja West	Non-conv.; carries TCSC
6	70	40–48	PH Main–Afam GS	Non-convergent
7	72	43–44	Itu–Eket	Non-convergent
8	73	43–46	Itu–Alaoji	Non-convergent

5. Discussion

On this network, wind-based active and reactive injection at the weakest bus outperformed TCSC series compensation on every loss and voltage metric examined: a 12.816% real power loss reduction against 0.396–0.589% for TCSC, a 3.034% reactive loss reduction against 0.335–0.777%, and voltage recovery at two of the three violating buses against one for TCSC. A real and reactive power source addresses the cause of loss and voltage droop directly, while a series FACTS device can only redirect existing power flow along the line [3]. The injection matches the broader pattern reported for renewable siting on this grid, where local injection has repeatedly outperformed transmission-level compensation for system-wide loss reduction as penetration increases [6].

Brown Bear Optimization and the Genetic Algorithm produced comparable objective values for both device types, with GA converging faster throughout and the two algorithms agreeing exactly on the wind solution. This agreement is a useful internal consistency check, suggesting a single, well-defined optimum within the searched bounds for that sub-problem. The BBO and GA selected different lines for TCSC placement, suggesting that the sub-problem is flatter or more multimodal by comparison; relying on a single algorithm for TCSC siting on this network should be aware that the reported optimum may not be unique.

The N-1 screening result is independent of this comparison and a more consequential finding for planning purposes: eight lines on the network violate part of the system on their own outage regardless of which device is installed, and one of these lines is the same line selected for TCSC placement, a coupling worth flagging to planners considering series compensation at that location. This is consistent with prior contingency work on the Nigerian grid showing that a small number of radial corridors dominate the network's exposure to severe single-line outages [13], and it means neither compensation strategy evaluated here confers meaningful N-1 security, however effective either is under intact-network conditions.

Kano's persistent violation under both compensation options (0.9471–0.9478 pu) needs further planning attention. This indicates a genuine northern reactive-support gap rather than a shortfall in either device's sizing, since both devices were sited to resolve the severe Sakete violation and neither reaches Kano electrically. Shunt reactive support (STATCOM or SVC) in the northern network would be a more direct remedy than resizing either device evaluated. The region's documented wind resource [14] remains an option is an option for future evaluation.

These results support three practical recommendations. First, transmission operators should prioritize localized renewable injection at high-demand terminal buses such as Sakete over series compensation alone. The substantially larger real-loss reduction achieved here (12.816% vs. <0.6%) is worth applying to a real-time network operation. Second, planning should move beyond single-device allocation toward co-optimized multi-device strategies to support multiple weak buses simultaneously. Third, infrastructure investment should be prioritized on the eight identified critical N-1 corridors, since no compensation device tested here changes their outage outcome; line-doubling or loop-closure on these radial branches addresses a vulnerability that no amount of optimal device siting can resolve.

This study's principal limitation is that BBO and GA are each reported as a single best run; repeating each search over multiple independent runs would let convergence statistics, rather than one result, support any operational adoption of either algorithm. A second limitation is that Kano's residual violation and the eight critical contingencies were not addressed by a second, independently sited device — a natural extension for future work, alongside a full techno-economic comparison that weighs each device's installed cost against its measured loss and voltage benefit.

References

[1] I. E. Nkan, O. I. Okoro, C. C. Awah, and U. B. Akuru, "Investigating the steady state stability of the Nigerian 48-bus systems using FACTS devices," Nigerian J. Technol. (NIJOTECH), vol. 38, no. 3, pp. 732–743, 2019.

[2] I. K. Okakwu, E. A. Ogujor, and P. A. Oriaifo, "Load flow assessment of the Nigeria 330-kV power system," Amer. J. Elect. Electron. Eng., vol. 5, no. 4, pp. 159–165, 2017.

[3] I. K. Okakwu, E. A. Ogujor, and P. E. Orukpe, "Improving the transient stability of the Nigeria 330kV transmission grid using thyristor controlled series compensator," Nigerian J. Technol., vol. 37, no. 4, pp. 1092–1098, 2018.

[4] M. Omoigui, O. A. Lawal, and R. A. Alao, "Improving the Nigerian 330kV power system steady state voltage stability using static VAr compensation and genetic algorithm optimization," Int. J. Eng. Emerg. Sci. Discovery, vol. 2, no. 2, pp. 1–25, 2017.

[5] T. T. Nguyen and F. Mohammadi, "Optimal placement of TCSC for congestion management and power loss reduction using multi-objective genetic algorithm," Sustainability, vol. 12, no. 7, Art. no. 2813, 2020.

[6] B. B. Adetokun, C. M. Muriithi, and J. O. Ojo, "Voltage stability assessment and enhancement of power grid with increasing wind energy penetration," Int. J. Elect. Power Energy Syst., vol. 120, Art. no. 105988, 2020.

[7] P. Kayal and C. K. Chanda, "Placement of wind and solar based DGs in distribution system for power loss minimization and voltage stability improvement," Int. J. Elect. Power Energy Syst., vol. 53, pp. 795–809, 2013.

[8] S. A. Adegoke, Y. Sun, A. S. Adegoke, and D. Ojeniyi, "Optimal placement of distributed generation to minimize power loss and improve voltage stability," Heliyon, vol. 10, no. 19, Art. no. e39298, 2024.

[9] A. Gacem et al., "Multi-objective sizing and location of DG in distribution network by hybrid gorilla troops optimization–genetic algorithm: a real case study," Sci. Rep., vol. 16, Art. no. 11334, 2026.

[10] T. Prakash, P. P. Singh, V. P. Singh, and S. N. Singh, "A novel brown-bear optimization algorithm for solving economic dispatch problem," in Advanced Control & Optimization Paradigms for Energy System Operation and Management. River Publishers, 2023, pp. 137–164.

[11] P. Mehta et al., "MOBBO: A multiobjective brown bear optimization algorithm for solving constrained structural optimization problems," J. Optim., vol. 2024, Art. no. 5546940, 2024.

[12] M. Nadeem, K. Imran, A. Khattak, A. Ulasyar, A. Pal, M. Z. Zeb, A. N. Khan, and M. Padhee, "Optimal placement, sizing and coordination of FACTS devices in transmission network using whale optimization algorithm," Energies, vol. 13, no. 3, Art. no. 753, 2020.

[13] E. F. Abul'Wafa, A. M. El'Garably, and M. Nasser, "Power system security assessment under N-1 and N-1-1 contingency conditions," Int. J. Eng. Res. Technol., vol. 12, no. 11, pp. 1854–1863, 2019.

[14] M. A. Sulaiman, I. K. Okakwu, A. S. Alayande, O. E. Olabode, and A. E. Ibhaze, "Wind energy evaluation and turbine identification for power generation in some selected areas in Nigeria," J. Eng. Stud. Res., vol. 26, no. 2, 2020.

[15] H. Saadat, (1999). *Power system analysis* (Vol. 2). New York: McGraw-hill.

[16] P. Kessel and H. Glavitsch, "Estimating the voltage stability of a power system," IEEE Trans. Power Del., vol. 1, no. 3, pp. 346–354, Jul. 1986.

[17] J. H. Holland, Adaptation in Natural and Artificial Systems. Ann Arbor, MI, USA: University of Michigan Press, 1975.

[18] G. C. Ejebe and B. F. Wollenberg, "Automatic contingency selection," IEEE Trans. Power App. Syst., vol. PAS-98, no. 1, pp. 97–109, Jan. 1979.

[19] N. T. Rao, K. K. Kumar, P. P. Kumar, R. S. S. Nuvvula, A. [24] N. H. Ikeli, C. E. Ashigwuike, and I. I. Alabi, "Investigation of the impact of PSO, ABC, BFO and Cuckoo search optimization techniques on UPFC device for sustainable voltage stability margin improvement," J. Electr. Syst. Inf. Technol., vol. 10, no. 1, pp. 1–21, 2023.

[25] C. S. Esobinenwu, "Comparative study on determination of voltage stability limits of the 330kV Nigerian power grid using four prediction optimizers," Int. J. Innov. Sci. Eng. Technol. Res., vol. 13, no. 3, pp. 25–39, 2025.

[26] C. S. Ezeonye, A. J. Atuchukwu, and I. I. Okonkwo, "Comparative effect of series and shunt FACTS on the steady state improvement of voltage profile of the Nigeria 330 kV transmission system," NIPES J. Sci. Technol. Res., vol. 6, no. 2, pp. 31–42, 2024.

[27] P. I. Obi, C. S. Ezeonye, A. A. Adeyi, I. K. Onwuka, and O. Oputa, "Investigating electricity power grid collapses in Nigeria and measures to reduce its effect during occurrence," NIPES J. Sci. Technol. Res., vol. 8, no. 1, pp. 197–211, 2026.

[28] K. C. Amadi, "Power system security optimization of the Nigerian 330kV transmission network," Innov. Energy Res., vol. 10, Art. no. 240, 2021.

[29] S. Gerbex, R. Cherkaoui, and A. J. Germond, "Optimal location of multi-type FACTS devices in a power system by means of genetic algorithms," IEEE Trans. Power Syst., vol. 16, no. 3, pp. 537–544, Aug. 2001.

Mutharasan, C. Dhanamjayulu, M. R. Shaik, and B. Khan, "Multiobjective optimal TCSC placement using multiobjective grey wolf optimizer for power losses reduction," Sci. Rep., vol. 14, Art. no. 21857, 2024.

[20] S. K. Ojha and C. O. Maddela, "Load frequency control of a two-area power system with renewable energy sources using brown bear optimization technique," Electr. Eng., vol. 106, pp. 3589–3613, 2024.

[21] A. W. Khawaja, N. A. M. Kamari, S. A. Halim, M. A. Zulkifley, S. Ansari, K. Khalid, and M. A. Khalil, "Enhancing power system stability using a TCSC-PIDF controller with innovative multiobjective function and hybrid optimisation logic," Sci. Rep., vol. 15, Art. no. 85325, 2025.

[22] A. A. Shehata, M. A. Tolba, A. M. El-Rifaie, and N. V. Korovkin, "Power system operation enhancement using a new hybrid methodology for optimal allocation of FACTS devices," Energy Rep., vol. 8, pp. 217–238, 2022.

[23] S. Mokred and Y. Wang, "Voltage stability assessment and contingency ranking in power systems based on modern stability assessment index," Results Eng., vol. 23, Art. no. 102548, 2024.

Table A1. Complete Base-Case Bus Voltage Solution — Nigeria 330 kV, 48-Bus Network**ppendix**

Bus No.	Bus Name	V (pu)	Angle (deg)	V (kV)	Violation
1	Birnin Kebbi	0.9908	1.1787	326.96	No
2	Kainji GS	1	1.9658	330	No
3	Kaduna	0.95588	-3.938	315.44	No
4	Kano	0.94711	-4.6719	312.55	Yes
5	Asaba	0.98518	-4.8996	325.11	No
6	Markudi	0.95297	-5.7135	314.48	No

Bus No.	Bus Name	V (pu)	Angle (deg)	V (kV)	Violation
7	Alagbon	0.99515	-11.868	328.4	No
8	Lekki	0.9871	-12.156	325.74	No
9	Jos	0.94955	-5.3841	313.35	Yes
10	Shiroro GS	1	0	330	No
11	Jebba	0.99639	-0.83496	328.81	No
12	Jebba GS	1	-0.59919	330	No
13	Oshogbo	0.9743	-4.6296	321.52	No

Bus No.	Bus Name	V (pu)	Angle (deg)	V (kV)	Violation
14	Ganmo	0.97625	-2.9855	322.16	No
15	Katampe	0.96477	-1.258	318.38	No
16	Gwagwalada	0.9756	-0.94797	321.95	No
17	Lokoja	0.97794	-1.0969	322.72	No
18	Ajaokuta	1.0002	-0.09675	330.07	No
19	Geregu GS	1	-0.017106	330	No
20	Odukpani GS	1	-1.6459	330	No
21	New Haven	0.98697	-4.7184	325.7	No
22	Ugwuaji	0.98233	-4.8984	324.17	No
23	Onitsha	0.98857	-4.6439	326.23	No
24	Benin	0.99604	-4.2046	328.69	No
25	Ihovbor GS	1	-3.8092	330	No
26	Adiabor	0.9939	-2.3472	327.99	No
27	Omotosho GS	1	-6.3472	330	No
28	Ayede	0.96969	-8.9211	320	No
29	Ikot Ekpene	0.97814	-4.1174	322.79	No
30	Olorunsogo GS	1	-9.2358	330	No
31	Sakete	0.92549	-14.666	305.41	Yes
32	Akangba	0.97207	-12.192	320.78	No
33	Ikeja West	0.97554	-11.924	321.93	No
34	Okearo	0.9872	-11.62	325.78	No
35	Aja	0.99954	-11.506	329.85	No
36	Egbin GS	1	-11.137	330	No
37	AES GS	1	-6.8264	330	No
38	Okpai GS	1	-2.4425	330	No
39	Sapele GS	1	-3.6507	330	No
40	PH Main	0.96091	-4.6398	317.1	No
41	Delta GS	1	-3.0338	330	No
42	Aladja	0.98888	-3.9629	326.33	No
43	Itu	0.97958	-5.9263	323.26	No
44	Eket	0.99	-6.7141	326.7	No
45	Ibom GS	1	-6.7259	330	No
46	Alaoji	0.97616	-4.3336	322.13	No
47	Alaoji GS	1	-1.3859	330	No
48	Afam GS	0.973	-3.5171	321.09	No